

PROPAGATION OF ACOUSTIC SIGNALS IN SOILS

Yu. A. Berezin¹ and L. A. Spodareva²

UDC 532.536

Propagation of low-amplitude waves in soils is studied within the framework of a hypoplastic model that describes the nonlinear behavior of grainy media. For one-dimensional disturbances, the original equations are reduced to a system of nonlinear wave equations. Results of the qualitative analysis and numerical solution of the problems are presented.

Many grainy materials, sand soils, in particular, are characterized by a nonlinear dependence between strains and stresses under loading and unloading. To describe their properties, hypoplastic models are used, in which the stress–strain relation is represented by a nonlinear evolution equation with coefficients depending, in the general case, on the stress-state parameters and porosity of the medium, and also on constants that characterize material types and are determined from experiments and calculations [1–4]. The results of studying some regularities of wave propagation in soils on the basis of such a model can be found in [5–10].

In the present work, the character of evolution of disturbances generated at the boundary of soil occupying a half-space is studied.

The main attention is paid to low-amplitude waves and small strains of the medium. Here, the effect of porosity is neglected, and the original system of equations is written in the following form:

$$\rho \dot{\mathbf{v}} = \operatorname{div} \mathbf{T}; \quad (1)$$

$$\dot{\mathbf{T}} = -\mathbf{T}\Omega + \Omega\mathbf{T} + f_1(\mathbf{T})\mathbf{D} + f_2(\mathbf{T}) \operatorname{tr}(\mathbf{T}\mathbf{D})\mathbf{D} + N(\mathbf{T})\|\mathbf{D}\|. \quad (2)$$

Here ρ is the density of the material, \mathbf{v} is the velocity vector, \mathbf{D} and Ω are the strain-rate and rotation tensors, respectively, $\|\mathbf{D}\| = \sqrt{\operatorname{tr}(\mathbf{D}\mathbf{D})}$ is the strain-rate tensor norm, $f_1(\mathbf{T}) = C_1 \operatorname{tr}(\mathbf{T})$, $f_2 = C_2/\operatorname{tr}(\mathbf{T})$, and $N(\mathbf{T}) = (C_3\mathbf{T}\mathbf{T} + C_4\mathbf{T}^*\mathbf{T}^*)/\operatorname{tr}(\mathbf{T}\mathbf{T})$, where $\mathbf{T}^* = \mathbf{T} - I \operatorname{tr}(\mathbf{T})/3$ (I is the unit tensor) and C_1, \dots, C_4 are empirical constants; the dot above the letter denotes the full derivative in time. The presence of the norm of the strain-rate tensor in the last term of Eq. (2), including all information on nonlinear properties of the model, does not allow linearization of system (1), (2) in the case of a homogeneous field of material velocities of the medium (in other words, in the vicinity of the value $\|\mathbf{D}\| = 0$). If the velocity distribution is inhomogeneous, linearization is possible.

Let us consider one-dimensional motions of a hypoplastic medium, assuming that the sought components of velocities and stresses are functions of one coordinate x and time t . We assume that the strains, material velocities, and deviations of the stress-tensor components from the undisturbed values are small. In addition, we consider the initial stress state as homogeneous and $\mathbf{v}^0 = 0$. (Hereinafter the superscript 0 corresponds to the initial undisturbed state of the medium.) Under these assumptions, system (1), (2) is reduced to the following system of three nonlinear second-order equations for the velocity components:

$$\begin{aligned} \frac{\partial^2 u}{\partial t^2} - c_p^2 \frac{\partial^2 u}{\partial x^2} &= a_1 \frac{\partial^2 v}{\partial x^2} + a_2 \frac{\partial^2 w}{\partial x^2} + b_1 \frac{\partial}{\partial x} \|\mathbf{D}\|, \\ \frac{\partial^2 v}{\partial t^2} - c_{s1}^2 \frac{\partial^2 v}{\partial x^2} &= a_3 \frac{\partial^2 u}{\partial x^2} + a_4 \frac{\partial^2 w}{\partial x^2} + b_2 \frac{\partial}{\partial x} \|\mathbf{D}\|, \end{aligned} \quad (3)$$

¹Institute of Theoretical and Applied Mechanics, Siberian Division, Russian Academy of Sciences, Novosibirsk 630090. ²Novosibirsk Military Institute, Novosibirsk 630117. Translated from *Prikladnaya Mekhanika i Tekhnicheskaya Fizika*, Vol. 42, No. 4, pp. 177–183, July–August, 2001. Original article submitted February 22, 2001.

$$\frac{\partial^2 w}{\partial t^2} - c_{s2}^2 \frac{\partial^2 w}{\partial x^2} = a_5 \frac{\partial^2 u}{\partial x^2} + a_6 \frac{\partial^2 v}{\partial x^2} + b_3 \frac{\partial}{\partial x} \|D\|.$$

Here

$$\|D\| = \sqrt{\left(\frac{\partial u}{\partial x}\right)^2 + \frac{1}{2}\left(\frac{\partial v}{\partial x}\right)^2 + \frac{1}{2}\left(\frac{\partial w}{\partial x}\right)^2}$$

and the coefficients c_p, c_{s1}, c_{s2}, a_i ($i = 1, \dots, 6$), and b_i ($i = 1, \dots, 3$) are determined by the parameters of the initial state of the medium and the model. If all the coefficients a_i and b_i are equal to zero, Eqs. (3) are transformed to linear wave equations independent of each other, which describe the propagation of three elastic waves (one longitudinal and two transverse) with velocities c_p, c_{s1} and c_{s2} , respectively. Assuming that the main axes of the undisturbed stress tensor T^0 coincide with the axes x, y , and z , so that $T_{xy}^0 = T_{xz}^0 = T_{yz}^0 = 0$, we obtain a simpler model

$$\frac{\partial^2 u}{\partial t^2} - c_p^2 \frac{\partial^2 u}{\partial x^2} = b \frac{\partial}{\partial x} \|D\|, \quad \frac{\partial^2 v}{\partial t^2} - c_{s1}^2 \frac{\partial^2 v}{\partial x^2} = 0, \quad \frac{\partial^2 w}{\partial t^2} - c_{s2}^2 \frac{\partial^2 w}{\partial x^2} = 0, \quad (4)$$

where

$$c_p^2 = \frac{1}{\rho} \left[C_1 \operatorname{tr}(T^0) + \frac{C_2 (T_{xx}^0)^2}{\operatorname{tr}(T^0)} \right], \quad c_{s1}^2 = \frac{1}{2\rho} [(C_1 + 1)T_{xx}^0 + (C_1 - 1)T_{yy}^0 + C_1 T_{zz}^0],$$

$$c_{s2}^2 = \frac{1}{2\rho} [(C_1 + 1)T_{xx}^0 + C_1 T_{yy}^0 + (C_1 - 1)T_{zz}^0], \quad b = \frac{1}{\rho \operatorname{tr}(T^0)} \left[C_3 (T_{xx}^0)^2 + \frac{C_4}{9} (2T_{xx}^0 - T_{yy}^0 - T_{zz}^0)^2 \right].$$

The first equation of system (4) is a nonlinear inhomogeneous wave equation that describes the longitudinal and transverse motions of the medium, and the other two are linear wave equations, as in the elastic case, with constant but, as a whole, different velocities c_{s1} and c_{s2} , since $c_{s1}^2 - c_{s2}^2 = (T_{zz}^0 - T_{yy}^0)/(2\rho)$. These velocities coincide only in the case $T_{yy}^0 = T_{zz}^0$. Thus, from system (4), it follows that two transverse (shear) waves propagate independent of each other and of the longitudinal motion, whereas the transverse motions affect the longitudinal waves. In other words, in hypoplastic media, the transverse waves lead to the excitation of longitudinal waves. If the initial stress state is isotropic ($T_{xx}^0 = T_{yy}^0 = T_{zz}^0 \equiv T_0$), then the expressions for wave-propagation velocities and the parameter of nonlinearity are sufficiently simplified: $c_p^2 = (3C_1 + C_2/3)T_0/\rho$, $c_{s1}^2 = c_{s2}^2 \equiv c_s^2 = 3C_1 T_0/(2\rho)$, and $b = C_3 T_0/(3\rho)$.

Then, all equations are written in dimensionless variables with the notation used for dimensional values. As is shown in [9, 10], in the absence of transverse motions ($v = w = 0$), the longitudinal disturbances, in which the material velocity coincides with wave-propagation direction, are described by the equation

$$\frac{\partial^2 u}{\partial t^2} - c_p^2 \frac{\partial^2 u}{\partial x^2} = b \frac{\partial}{\partial x} \left| \frac{\partial u}{\partial x} \right|. \quad (5)$$

The solution of this equation depends on the sign of the derivative $\partial u/\partial x$. Indeed, if we have $\partial u/\partial x > 0$ everywhere, then Eq. (5) reduces to the linear wave equation

$$\frac{\partial^2 u}{\partial t^2} - (c_p^2 + b) \frac{\partial^2 u}{\partial x^2} = 0,$$

and its solutions correspond to the transfer of the initial disturbance in both directions of the x axis, without changing its form, with a constant velocity $c_1 = \pm \sqrt{c_p^2 + b}$. If we have $\partial u/\partial x < 0$ everywhere and $b < c_p^2$, then eq. (5) takes the form

$$\frac{\partial^2 u}{\partial t^2} - (c_p^2 - b) \frac{\partial^2 u}{\partial x^2} = 0,$$

and its solutions describe the transfer of the initial disturbances, without changing their form, with a constant velocity $c_2 = \pm \sqrt{c_p^2 - b}$. In the hydrostatic case considered, when shear stresses are absent, the parameter b is positive; therefore, $c_1 > c_2$ and the profiles corresponding to the positive values of the velocity gradient propagate faster than the profiles with the negative values of this gradient.

Note that Eq. (5) apart from longitudinal waves, describes also low-amplitude shear waves in saturated grainy media [5–7]. The sought function is the transverse velocity v ; the coefficients differ from those mentioned above.

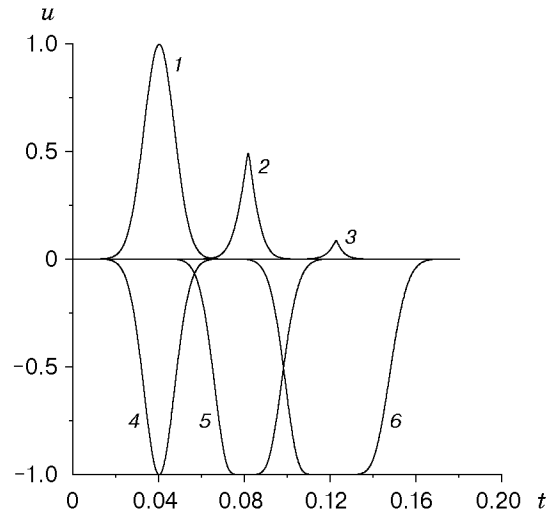


Fig. 1. Evolution of a single signal (transfer equation) for $u_0 = 1$ (1-3) and $u_0 = -1$ (4-6): curves 1 and 4, 2 and 5, and 3 and 6 refer to $x = 0, 0.02$, and 0.04 , respectively.

If the parameter of nonlinearity b is small as compared to the value of c_p^2 , the following first-order equation was obtained for waves propagating in the positive direction of the x axis, using approximate factorization of the wave operator [9]:

$$\frac{\partial u}{\partial t} + c_p \frac{\partial u}{\partial x} + \frac{b}{2c_p} \left| \frac{\partial u}{\partial x} \right| = 0. \quad (6)$$

In [9, 10], a numerical solution of Eq. (6) on a dimensionless straight line $-\infty < x < \infty$ with the initial spatially localized velocity distribution and zero boundary conditions is presented. It is shown that, since the initial profile has two branches with different signs of the velocity gradient, they move in the same direction with different velocities, the fore front moves slower than the rear front. Their interaction leads to a decrease in the disturbance amplitude in the process of motion, and this disturbance decays completely with time. If Eq. (6) is solved under the same conditions but with the negative sign of c_p , in this case, the fore front of the disturbance moves faster than the rear front, and the branches with different signs of the velocity gradient move not interacting with each other; because of this, the disturbance is expanded in the course of time, the amplitude remaining unchanged.

On the basis of the approximate equation (6), we consider the propagation of longitudinal waves in soil occupying a half-space $x > 0$. The waves are generated by pulses $u(0, t) = f(t)$ prescribed at the boundary $x = 0$. Let a vibrating source generate a single signal

$$f(t) = u_0 \exp \left[- \left(\frac{t - t_0}{t_1} \right)^2 \right],$$

where u_0 is the amplitude, t_0 is the time of reaching the maximum value, and t_1 is the duration of the signal. This pulse leads to the excitation of loading ($u > 0$) or unloading ($u < 0$) waves, which depends on the positive or negative value of u_0 . Figure 1 shows the dependence of the medium velocity on time at the boundary $x = 0$ and at two points $x_1 > 0$ and $x_2 > 0$. These curves may be interpreted as a temporal development of signals, recorded by sensors located in the soil at a certain distance from the source. Curves 1-3 correspond to medium loading ($u_0 > 0$), where the fore front velocity is smaller than the rear front velocity. The sensors record the signal of decreasing amplitude with increasing distance from the source, and the signal decays completely at rather large distances. Curves 4-6 correspond to soil unloading ($u_0 < 0$), the fore front velocity of the signal is higher than the rear front velocity, the disturbance moves in the medium without decaying, and its duration increases.

We consider the case where the vibrating source generates a sinusoidal signal of a constant amplitude $f(t) = u_0 \sin \omega t$ (ω is the cyclic frequency related to the frequency period as $T = 2\pi/\omega$). Figure 2 shows the temporal development of signals recorded by the sensors at the points $x_1 > 0$ and $x_2 > 0$ in the soil. As it follows from the analysis of Fig. 2, the sinusoidal pulse changes substantially during its propagation. In regions under loading, the velocity profiles are sharpened, and their amplitude decreases (as in the case of generating a single loading signal at the soil boundary), whereas the velocity profiles in unloading regions are expanded at an invariable

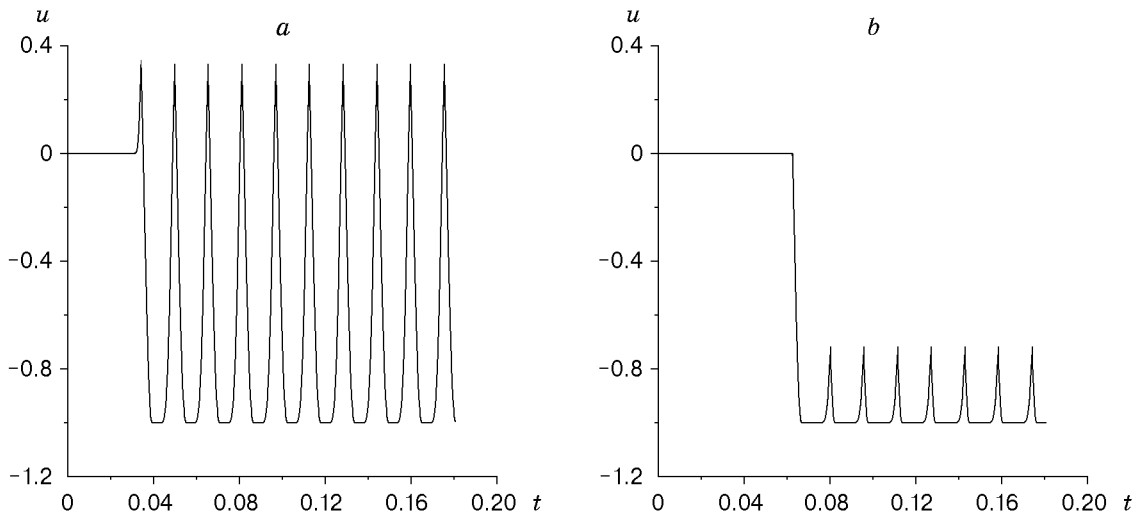


Fig. 2. Evolution of a sinusoidal signal (transfer equation) for $x = 0.01$ (a) and 0.02 (b).

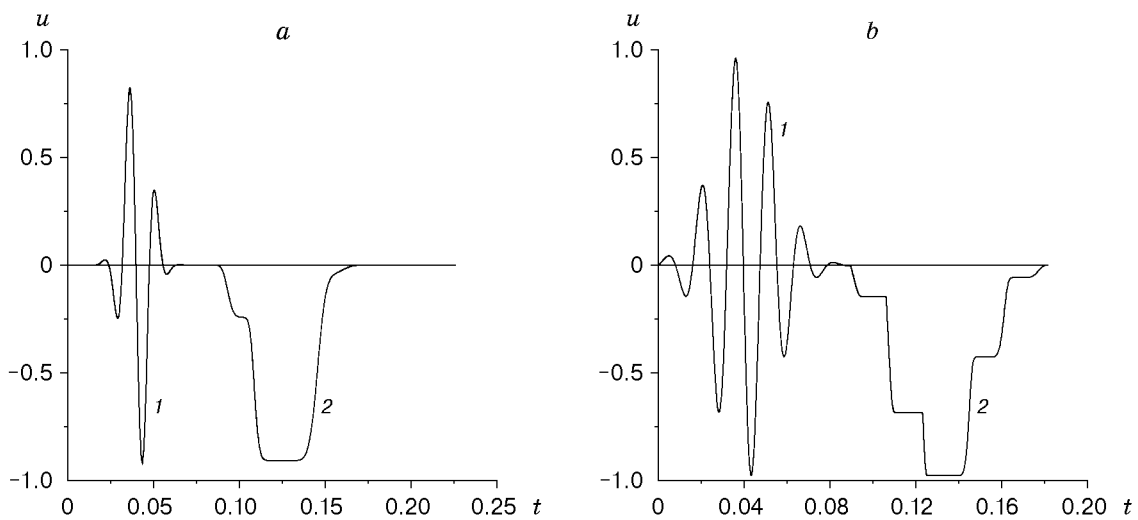


Fig. 3. Evolution of a decaying sinusoidal signal (transfer equation) for $t_1 = 0.01$ (a) and 0.02 : curves 1 and 2 refer to $x = 0$ and 0.04 , respectively.

amplitude (as in the case of a single pulse of rarefaction). Such a change in the pulse form leads to the formation of a signal of greater duration, corresponding to unloading of the medium.

If the source generates a sinusoidal pulse of finite duration with a decreasing amplitude

$$f(t) = u_0 \exp \left[- \left(\frac{t - t_0}{t_1} \right)^2 \right] \sin \omega t,$$

the signal form $u(x, t)$ in the course of penetration changes in the following manner. In regions under loading, the velocities decrease with time, decaying completely at large times; but the velocity profiles are expanded in regions under unloading, the amplitude remaining unchanged. Moreover, as the pulse amplitude decreases at the boundary, the maximum values of velocity in the successive regions under unloading are different; as a result, the pulse acquires a stepwise form at large distances from the source (Fig. 3). The number of steps is equal to the number of regions under unloading, which is set by the pulse at the boundary. Note that the pulse duration in Fig. 3b is twice as large as in Fig. 3a.

The first-order equation (6) is obtained using approximate factorization of the wave equation (5). Let us compare the results of the numerical solution of these equations. Figure 4 shows the temporal developments of the signal generated by a single pulse at the soil boundary $x = 0$ at the same points and at the same parameters that were used in solving the first-order equation. It is seen that the character of the signal is the same as in Fig. 1. In

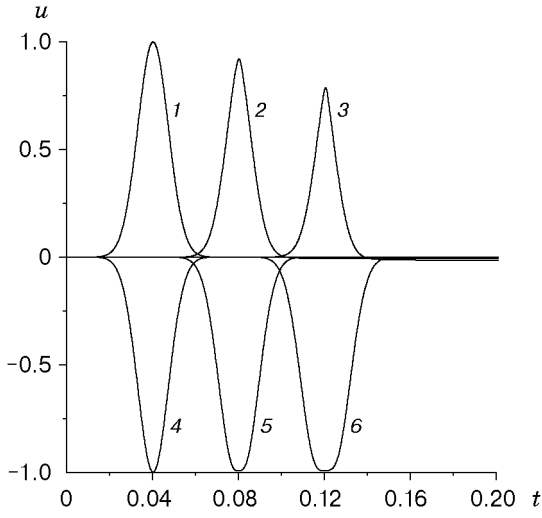


Fig. 4

Fig. 4. Evolution of a single signal (wave equation) for $u_0 = 1$ (1-3) and $u_0 = -1$ (4-6): curves 1 and 4, 2 and 5, and 3 and 6 refer to $x = 0, 0.02,$ and $0.04,$ respectively.

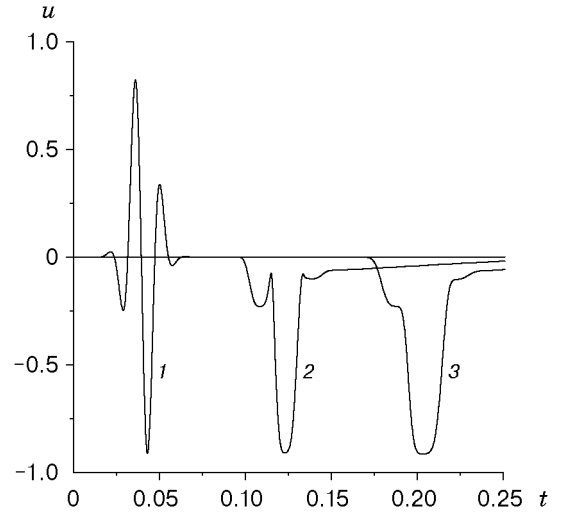


Fig. 5

Fig. 5. Evolution of a decaying sinusoidal signal (wave equation) for $x = 0$ (1), 0.04 (2), and 0.08 (3).

the course of penetration into the medium, the signal under loading becomes sharper and its amplitude decreases (curves 1–3 in Fig. 4); under unloading, the signal duration increases, but the amplitude remains constant (curves 4–6). However, the process of development simulated by the wave equation (5) is slower than that described by Eq. (6). Besides, in the course of penetration, the signal takes a long “tail” of low amplitude, corresponding to unloading ($u < 0$), which is absent in simulating the process by Eq. (6). When the sensor is far from the source, the signal character indicates a gradual decrease in the loading region size and an increase in the unloading region size. The sensor located at a large distance from the soil boundary records a long signal corresponding to unloading.

Figure 5 shows the results of the numerical solution of the wave equation (5), when the source at the boundary generates a sinusoidal signal of decreasing amplitude and, hence, finite duration. All parameters in the calculation of signal development are identical (see Figs. 3a and 5), which allows us to compare the results obtained by solving two equations: the wave equation (5) and the transfer equation (6). From the comparison of Eqs. (5) and (6), it is seen that the character of signal propagation is qualitatively identical: at large distances from the source, the sensor records a signal corresponding to unloading ($u < 0$), and the number of steps on the temporal development is equal to the number of unloading regions, which depends on the pulse character at the boundary $x = 0$. However, the process described by the wave equation develops considerably slower than the process simulated by the transfer equation.

For the numerical solution of Eq. (5), a double-layer explicit scheme [9] was used, in which the derivative on the coordinate is approximated by the backward difference for the reason of stability, because the coefficient before the derivative on the coordinate is always positive and equal to either $c_p + b/(2c_p)$ for $u_x > 0$ or $c_p - b/(2c_p)$ at $u_x < 0$ ($0 < b < c_p$). Equation (5) was solved numerically by the scheme used in [10]. Equation (5) is written in the form of the system of two first-order equations for the velocity and stress

$$\frac{\partial T}{\partial t} = c_p^2 \frac{\partial u}{\partial x} + b \left| \frac{\partial u}{\partial x} \right|, \quad \frac{\partial u}{\partial t} = \frac{\partial T}{\partial x},$$

where $T \equiv T_{xx} - T_0$. For this system, an implicit finite-different scheme is constructed, which is implemented by successive approximations:

$$T_i^{n+1,k+1} = T_i^n + (c_p^2 \delta t / \delta x) [\alpha (\Delta u_i^n + b |\Delta u_i^n|) + (1 - \alpha) (\Delta u_i^{n+1,k} + b |\Delta u_i^{n+1,k}|)],$$

$$u_i^{n+1,k+1} = u_i^n + (\delta t / \delta x) [\alpha \Delta T_i^n + (1 - \alpha) \Delta T_i^{n+1,k}].$$

Here $T_i^n = T(t_n, x_i)$, $u_i^n = u(t_n, x_i)$, $\Delta T_i^n = T_{i+1}^n - T_i^n$, $\Delta u_i^n = u_i^n - u_{i-1}^n$, $\Delta T_i^{n+1,k} = T_{i+1}^{n+1,k} - T_i^{n+1,k}$, and $\Delta u_i^{n+1,k} = u_i^{n+1,k} - u_{i-1}^{n+1,k}$ (k is the iteration number), the parameter $\alpha = 1$ corresponds to the explicit scheme,

$0 \leq \alpha < 1$ to the implicit scheme, and δt and δx are the grid steps in time and coordinate, respectively. The iterations are conducted until the difference in the values of the sought functions on two successive iterations becomes smaller than some small number ε .

The calculation results presented in Figs. 1-5 are performed for the following parameters: $b = 0.1$, $c_p = 0.5$, $t_0 = 0.04$, $\alpha = 0.2$, $\delta t = 0.0001$, and $\delta x = 0.0002$. For the sinusoidal signals (see Figs. 2, 3, and 5), we have $\omega = 400$.

This work was supported by the Russian Foundation for Fundamental Research (Grant No. 00-05-65337).

REFERENCES

1. D. Kolymbas, "An outline of hypoplasticity," *Arch. Appl. Mech.*, **61**, 143–151 (1991).
2. G. Gudehus, "A comprehensive constitutive equation for granular materials," *Soils Found.*, **36**, No. 1, 1–12 (1996).
3. D. Kolymbas, S. V. Lavrikov, and A. F. Revuzhenko, "Method of analysis of mathematical models of media under complex loading," *Prikl. Mekh. Tekh. Fiz.*, **40**, No. 5, 133–142 (1999).
4. D. Kolymbas, *Introduction to Hypoplasticity*, Balkema, Rotterdam (2000).
5. V. A. Osinov and G. Gudehus, "Plane shear waves and loss of stability in a saturated granular body," *Mech. Cohesive-Frict. Mater.*, **1**, 25–44 (1996).
6. M. S. Gordon, M. Shearer, and D. Schaeffer, "Plane shear waves in a fully saturated granular medium with velocity and stress controlled boundary conditions," *Int. J. Nonlinear Mech.*, **32**, No. 3, 489–503 (1997).
7. B. T. Hayes and D. G. Schaeffer, "Plane shear waves under a periodic boundary disturbance in a saturated granular medium," *Physica D*, **121**, 193–212 (1998).
8. V. A. Osinov, "Theoretical investigation of large-amplitude waves in granular soils," *Soil Dyn. Earthquake Eng.*, **17**, 13–28 (1998).
9. Yu. A. Berezin and L. A. Spodareva, "Longitudinal waves in grainy media," *Prikl. Mekh. Tekh. Fiz.*, **42**, No. 2, 148–152 (2001).
10. Yu. A. Berezin, V. A. Osinov, and K. Hutter, "Evolution of plane disturbances in hypoplastic granular materials," *Continuum Mech. Thermodyn.*, **13**, 25–40 (2001).